A COMPARATIVE PERFORMANCE ANALYSIS OF VIENNA RECTIFIER AND INTELLIGENT CONTROLLED SEPIC FOR WIND ENERGY CONVERSION SYSTEM

Muthukumari.T [1], Kalaivani.R[2], Raghavendiran.T.A[3]
[1]Research scholar, Department of Electrical and Electronics Engineering, Anna University, Chennai, India.
[2]Department of Electrical and Electronics Engineering, Rajalakshmi Engineering College, Chennai, India.
[3]Department of Electrical and Electronics Engineering, Anand Institute of Higher Technology, Chennai, India.
E-mail: muthukumari123@yahoo.co.in, kalaivani.r@rajalakshmi.edu.in, taraghavendiran@yahoo.co.in

Abstract: *This paper presents a PMSG based variable speed wind energy generating system using Vienna rectifier for conversion of AC to DC supply. A DC-DC Single-Ended Primary Inductor converter (SEPIC) was used in closed loop control to maintain the output voltage of grid connected inverter constant. The quality of output power is maintained as per the International Electro Commission standard IEC61400 which determines the output performance of the wind turbine generator. In order to achieve the aforementioned objective, the generated power from the wind source is converted from AC to DC, fixed DC to variable DC and then variable DC to AC. The quality of power is attained by maintaining the input of grid connected inverter (output of SEPIC converter) constant by operating the SEPIC converter in closed loop with controller. This paper presents the closed loop operation of SEPIC converter with proposed ANFIS (adaptive Neuro-fuzzy inference system) tuned PID controller implemented using Matlab/Simulink. The results obtained reveal that the proposed controller reduces the transient performance indices such as settling time, rise time and overshoot and also reduces THD of the system than the conventional PID controller and Fuzzy tuned PID controller. Moreover, the proffered controller increases the efficiency of the overall system than the conventional controller.*

Keywords: *Vienna rectifier, Single Ended Primary Inductor converter, adaptive Neuro-fuzzy inference system, Power Quality and Total Harmonic Distortion.*

1. Introduction

In the last two decades wind energy has evolved as one of the prominent renewable energy sources. The number of wind power production systems installed has increased in India as well as around the world. Due to remarkable reduction in the production of wind power and advancement in technologies has contributed to large scale electric power production systems. In another five years wind power generation is expected to increase to 1.26 million of MW which will cover 12% of electric power consumption worldwide [1].

There are two types of wind turbines, one is fixed speed and other one is a variable speed wind turbine. Out of these, Variable Speed Wind turbine provides large scale power generation, and is widely preferred. It uses a power converter to provide better controlling capacity when compared to fixed speed wind turbine. It has gained its importance over other wind power generation systems due to its higher power extraction efficiency as well as quality of power [2-3].

Renewable energy resources such as solar and wind are losing their popularity for the reason that climatic and weather changes are unpredictable. Fluctuations in the output electric power generated from such resources may results in large variations in the frequency and amplitude of signals to the grid. To avoid fluctuations and to improve the quality of power, Power Electronic (PE) interface can be used for conversion and control of electric power. Depending on the type of renewable energy source and requirement of load, the Power electronic converter is selected.

For a wind energy generation system, a single stage AC-DC conversion or AC-AC conversion or multi stage AC-DC-AC conversion can be implemented. Back to back full scale power converters are utilized in PMSG based WECS at generator side and grid side converters for interfacing with the power system. At the generator side, uncontrolled three phase diode rectifiers and six switch two level PWM converters can be used [4 -5]. The distortion in generator current is very high with the use of diode rectifier and hence three phase, three switch, three level PWM Vienna rectifier converter is preferred [6]. Vienna rectifier uses three power switches and generate three voltage levels their by reducing the production cost ,providing power quality enhancement, reliability and reduced blocking voltage stress on the power semiconductors. When operating a PMSG at lagging power factor, large reactive power is generated at the stator terminals and hence the active power is largely reduced. It is essential to maintain a high power factor and good

quality current at the generator side. So a converter with better current control ability is required.

Depending on the type of application a suitable DC-DC converter is implemented to modulate the input voltage. Various types of DC -DC converters such as isolated DC–DC converter and non-isolated DC–DC converter are available. Reduction in cost and simple design can be achieved with buck–boost, cuk, Luo and SEPIC non isolated DC-DC converters. In the proposed system SEPIC is used because it leads to distortion less output current, lesser ripple and low switching stress [7]. By implementing SEPIC the overall cost of the system is reduced due to absence of high frequency filters.

While designing converters, conduction, switching losses and output current ripple are critical factors which can be minimized by implementing either conventional controllers such as PI, PID or intelligent controlling techniques [8-9].

In order to have better sturdiness different Intelligent or soft switching techniques like Fuzzy Logic control, Artificial Neural Network and ANFIS control can be used [10-11]. In this paper the PID controller is tuned by applying intelligent methods based on fuzzy logic and ANFIS controller. The performance of methods based on fuzzy logic and ANFIS controller is compared an analyzed. The proposed intelligent methods when related to conventional methods provide improved performance.

The DC voltage obtained from SEPIC is converted into AC of constant voltage and frequency (415 V, 50 Hz) using a three phase multilevel inverter. This paper is organized as follows: Section 2 presents the overall system description. Section 3 illustrates the different controllers used with SEPIC. Section 4 presents the Simulation results and its analysis. The conclusion is presented in Section 5.

2. Overall system description

The schematic block diagram of the system is shown in Fig 1. It consists of the 1 kW Wind Turbine, Permanent Magnet Synchronous Generator, and Vienna Rectifier, SEPIC along with a Controller, Multilevel Inverter, Transformer and Load.

A PMSG generates and delivers the AC voltage to the three-phase Vienna rectifier which converts AC to DC. The uncontrolled DC output from Vienna rectifier is fed to the SEPIC. During wind speed variations, the output voltage of the SEPIC is controlled by tuning conventional or soft switching controller. Then DC is converted into AC (415 V, 50 Hz) using a three phase multilevel inverter which is then fed to utility grid or load.

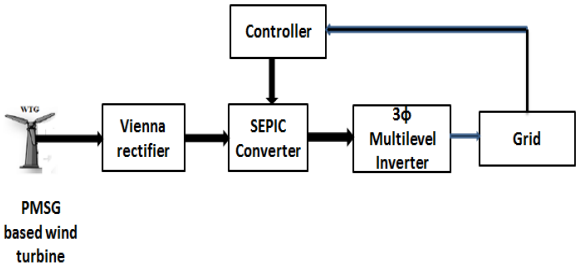

Fig. 1 Block diagram of PMSG based WECS

2.1 Wind energy systems

Wind energy conversion system (WECS) converts kinetic energy in to mechanical energy by means of wind turbine rotor blades and the generator converts the mechanical energy in to electrical energy.

2.1.1 .Turbine model

The components of a typical wind energy conversion system consist of wind turbine blades, a generator (Permanent Magnet Synchronous Generator), control system and equipments for interconnection. It makes the conversion system as a complex one. The power available in a uniform wind field can be expressed as in [17],

$$P_m = 0.5\, C_p(\lambda,\beta)\, \rho\, A\, V^3 \quad (1)$$

Where, A is the swept area in m^2, V is the Wind speed in m/sec, C_p is the Power coefficient, β is the Pitch angle in degrees, and λ is the Tip Speed Ratio.

The power coefficient of the wind turbine is expressed as

$$C_p(\lambda,\beta) = C_1\left(\frac{C_2}{\lambda_i} - C_3\beta - C_4\right)e^{\frac{-C_5}{\lambda_i}} + C_6\lambda \quad (2)$$

$$\frac{1}{\lambda_i} = \left[\frac{1}{\lambda + 0.089} - \frac{0.035}{\beta^2 + 1}\right] \quad (3)$$

The coefficients C_1 to C_6 are: C_1=0.5176, C_2=116, C_3=0.4, C_4=5, C_5=21 and C_6=0.0068.

Variation of Power coefficient C_p for the wind turbine used in this study with respect to tip speed ratio is represented as a plot in Fig. 2 for different values of blade pitch angle β.

It is seen that the optimum or maximum value of power coefficient C_p is achieved at β = 0. Fig. 3. Shows the turbine power characteristics, is plotted between turbine speed and turbine output power displaying the default parameters (base wind speed =

12 m/s, maximum power at base wind speed = 0.73 p.u. and base rotational speed = 1.2 p.u.).

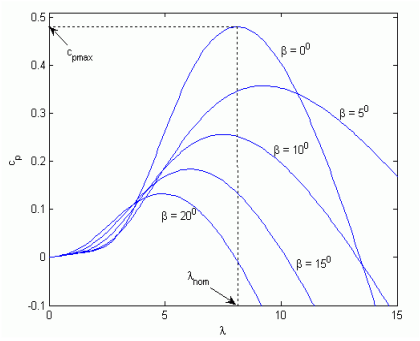

Fig. 2. Wind turbine power coefficients C_p as function of λ and β

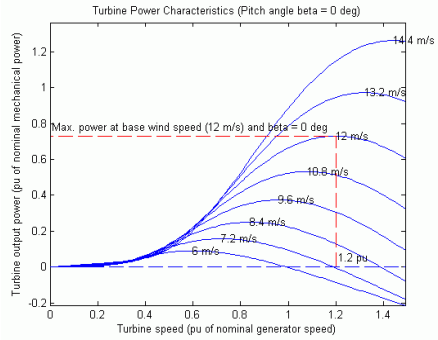

Fig. 3. Turbine power characteristics

2.1.2. PMSG model

In a PMSG, the field winding of the rotor is replaced by a permanent magnet. Hence, the elimination of field copper loss, high power density, less rotor inertia, and more robustness is achieved. The drawbacks are loss of flexibility in field flux control, demagnetization effect and cost. The modeling of the PMSG is similar to the classical synchronous machine. The PMSG is designed considering sinusoidal-distributed windings neglecting saturation, eddy currents, and hysteresis losses.

The dynamic equations (10)-(11) of a three-phase PMSG can be expressed in the rotating d–q reference frame as shown below

$$L_d \frac{di_{sd}}{dt} = -u_{sd} + L_q n w_m i_{sq} - R_s i_{sd}$$
$$L_q \frac{di_{sq}}{dt} = -u_{sq} + L_d n w_m i_{sq} - R_s i_{sq} + n w_m \psi_f \quad (4)$$

Where u_{sd} and u_{sq} are the stator voltages in the direct and quadrature axis of rotor respectively. i_{sd}, i_{sq} are stator currents in d and q axis, R_s is phase resistance of stator, L_d and L_q are the stator inductances, ψ_f is the magnetic flux and n is the pair of poles=ω_m.n where ω_m is the rotor speed [12].

The electromagnetic torque T_e is represented as

$$T_e = \frac{3}{2} \psi_f i_{sq} \quad (5)$$

The rotor dynamics of PMSG can be given as

$$J \frac{dw}{dt} = T_m - T_e - B W_m \quad (6)$$

Where J is the total inertia (kgm^2), B is viscous friction coefficient (kgm^2/s), and T_m is the drive torque produced by the wind (N-m).

The expressions for active and reactive powers of PMSG in steady state conditions are given below,

$$P_s = u_{sd} i_{sd} + u_{sq} i_{sq}$$
$$Q_s = V_{sq} i_{sd} - v_{sd} i_{sq} \quad (7)$$

2.2. Vienna rectifier

Vienna rectifier is selected for the system replacing diode rectifier to increase output power but curbing the increase in the losses for AC - DC conversion. It is a three phase, three levels and three-switch rectifier. It provides a partly controlled output DC voltage.

The topology of the Vienna Rectifier is shown in Fig. 4. It is a combined form of a boost DC-DC converter with a three-phase diode bridge rectifier. The output capacitor is divided into two equal values (C_1 and C_2). Voltages $+V_0/2$ and $-V_0/2$ are obtained across the capacitors respectively Hence three different voltages ($+V_0/2$, 0, $-V_0/2$) are offered. The main disadvantages of Vienna rectifier is large number of diodes [13].

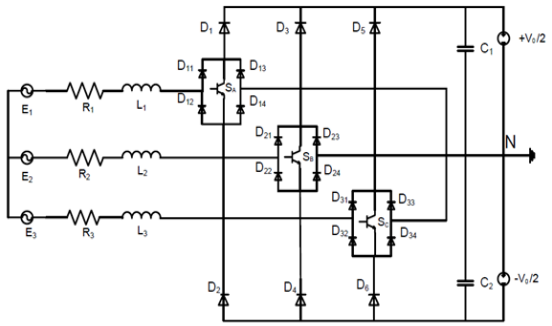

Fig. 4.Topology of Vienna rectifier

It has three switches and depending on the direction of the current in each phase, the voltage is obtained by selecting the ON/OFF state in each switch. In this circuit, the center point N represents zero voltage. The phase voltage is expressed as,

$$V_{pn} = E_n - L_n \frac{di_p}{dt} \quad (8)$$

Where L_n are the input inductors (n=1, 2, 3), i_p is the input phase current.
When the phase current is positive,

$$V_{pn} = \begin{cases} +V0/2, & sw = 0 \\ 0, & sw = 1 \end{cases} \quad (9)$$

When the phase current is negative,

$$V_{pn} = \begin{cases} -V0/2, & sw = 0 \\ 0, & sw = 1 \end{cases} \quad (10)$$

V_{pn} is the phase voltage (p =A, B, C), sw is a controlled switch (sw= 0 correspond to off state and sw = 1 correspond to the on state).

2.3. SEPIC

The SEPIC is a type of non-isolated DC-DC converter. It can step up and step down the input voltage as well keeping the voltage constant [14]. The main drawbacks of SEPIC converter are the conduction, switching losses and output ripple current. This problem can be addressed by using intelligent switching technique. Fig.6 shows the basic circuit model of SEPIC converter.

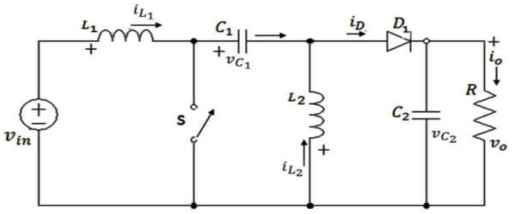

Fig.6. Basic circuit model of SEPIC converter.

It has two coupled inductors L_1 and L_2, an output capacitor, C_2,a coupling capacitor, C_1,a power switch (FET) S, and a diode D_1.When switch S is turned off, the voltage across inductor L_2 will be V_o. When switch S is turned on, capacitor C_1 is charged to input voltage V_{in}, and hence the voltage across L_2 is $-V_{in}$.While Switch is on, magnetic energy is stored in inductor L_1 from input voltage and energy is L_2 is stored from C_1.While Switch is off, the current flowing through L_1 also flows through C_1 and D_1 then into C_2 on the load. The relation between input and output currents and voltage are expressed below

$$\frac{V_0}{V_{in}} = \frac{D}{1-D} \quad (11)$$

$$\frac{I_{in}}{I_0} = \frac{D}{1-D} \quad (12)$$

The SEPIC converter duty cycle under continuous conduction mode is given by

$$D = \frac{V_{out} + V_D}{V_{in} + V_{out} + V_D} \quad (13)$$

Where V_D is the forward voltage drop across the diode (D1).
The maximum duty cycle is

$$D_{\max} = \frac{V_{out} + V_D}{V_{in(\min)} + V_{out} + V_D} \quad (14)$$

The value of the inductor is chosen based on the following equation

$$L_1 = L_2 = L = \frac{V_{in(\min)} * D_{\max}}{\Delta I_i * f_{sw}} \quad (15)$$

ΔI_i is the peak-to-peak value of ripple current at the minimum input voltage and f_{sw} is the switching frequency. The value of C_2 depends on RMS current, which is given by

$$I_{c2(rms)} = I_{out} * \sqrt{\frac{V_{out} + V_D}{I_{in(\min)}}} \quad (16)$$

The voltage rating of capacitor C_2 must be greater than the input voltage. The ripple voltage on C_2 is given by

$$\Delta V_{c1} = \frac{I_{out} * D_{\max}}{C_1 * fsw} \quad (17)$$

3.Control scheme of SEPIC

3.1.Fuzzy logic controller

Fuzzy logic controller has gained significant importance recently. It provides a good logical response to the varying input parameters. Tagachi-Sukeno (T-S) and Mamdani are two design methods available in Fuzzy Logic Controller, of which Mamdani method is used in proposed model [15] Fig. 7.shows the block diagram for the fuzzy logic controller.

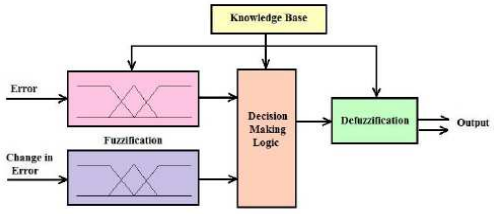

Fig. 7.Block diagram for fuzzy logic controller

FLC process comprises of fuzzification, rule base with fuzzy inference system and defuzzification process. Fuzzification includes conversion of exact

input values into fuzzy values and processes the values as per the rule base using fuzzy inference system. Then Fuzzy values are converted back into exact values using defuzzification. The proposed model requires two input variables error and change of error to control two output variables. The ranges of these inputs are from -1 to 1 .The input and output variables have seven membership functions namely VN (very Negative), MN (Medium Negative), SN (Small Negative), Z(zero), SP (small Positive), MP (Medium Positive), VP (Very Positive). The membership functions of these inputs 1, 2 fuzzy sets are shown in Fig. 8 and Fig.9. The membership functions of output 1 and 2 is shown in Fig. 10 and Fig.11.

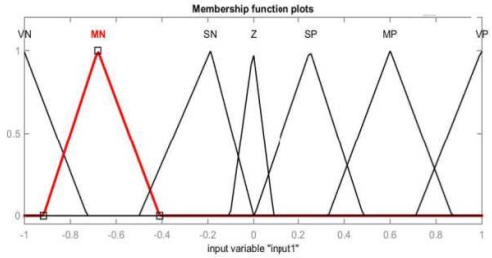

Fig. 8.Input 1 membership function

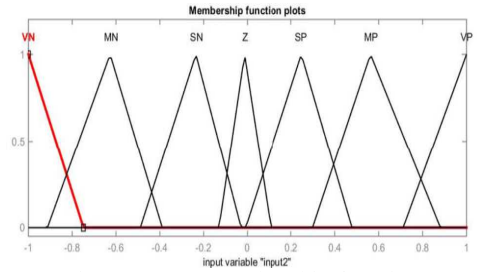

Fig. 9.Input 2 membership function

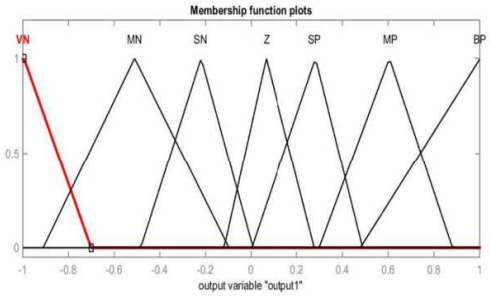

Fig. 10.output 1 membership function

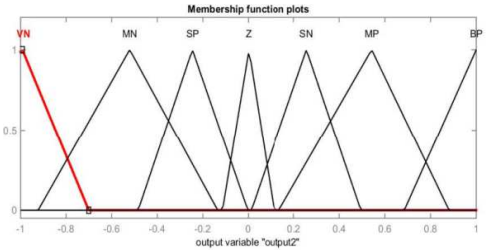

Fig. 11.Output 2 membership function

The rules base for the fuzzy-PID controller is shown in Table1 and Table 2 which can be implemented for tuning the PID controller.

Table 1. Rule base for fuzzy-PID controller (output1)

error	Derivative of error						
	VN	MN	SN	Z	SP	MP	VP
VN	VP	VP	MP	SP	SP	Z	SN
MN	MP	MP	MP	SP	SP	Z	SN
SN	MP	MP	MP	SP	Z	SN	SN
Z	MP	MP	SP	Z	SN	MN	MN
SP	SP	SP	Z	SN	SN	MN	MN
MP	SP	Z	SN	MN	MN	MN	BP
VP	Z	SN	MN	MN	MN	VN	VN

Table 2. Rule base for fuzzy-PID controller (output2)

error	Derivative of error						
	VN	MN	SN	Z	SP	MP	VP
VN	VN	VN	MN	MN	SN	SN	Z
MN	VN	VN	MN	SN	SN	Z	SP
SN	VN	MN	SN	SN	Z	SP	SP
Z	MN	MN	SN	Z	SP	MP	MP
SP	MN	SN	Z	SP	SP	MP	BP
MP	SN	Z	SP	SP	MP	VP	BP
VP	Z	SP	SP	MP	MP	VP	BP

The Rule Viewer of the Fuzzy Logic Controller is as shown in Fig.12.

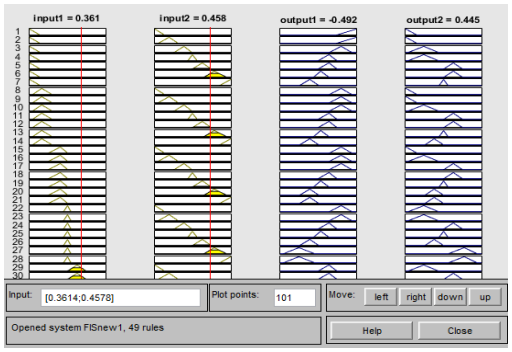

Fig. 12.Rule viewer of fuzzy logic controller

The Surface Viewer of the Fuzzy Logic controller is shown in Fig.13 and Fig. 14.

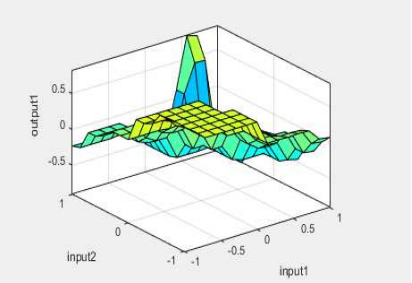

Fig.13.The Surface Viewer of the FLC (output 1)

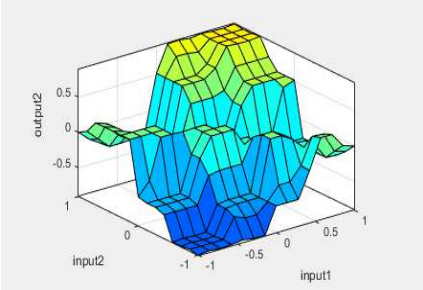

Fig.14.The Surface Viewer of the FLC (Output 2)

The Simulink block set for fuzzy PID controller implemented is shown in Fig. 15.

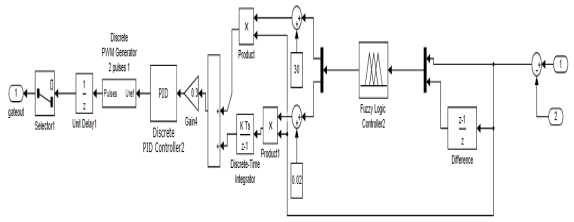

Fig 15.Fuzzy-PID controller implementation in MATLAB Simulink

3.2.Adaptive neuro-fuzzy inference system

A hybrid system comprised of both neural network and fuzzy logic properties is known as Neuro fuzzy networks.ANFIS(Adaptive Neuro-Fuzzy Inference System) is such a neuro fuzzy network which can learn easily from the input data as done by neural network.It also utilises the simplicity of fuzzy logic since verbal terms are used in place of numbers[16]. ANFIS consists of three main parts: auxiliary, compatible and integrative. Triangle type membership functions were used for the inputs and the outputs of the fuzzy inference system. A general block diagram of ANFIS controller system structured for two-rule fuzzy system is given in Fig.16.

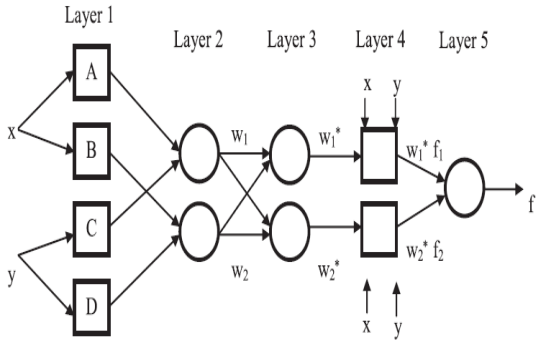

Fig. 16.Schematic diagram of ANFIS

Two fuzzy if-then rules from Takagi-Sugeno (TS) model are expressed as:

Rule 1: If (X is A_1) and (Y is B_1) then

$$f_1 = p_1X + q_1Y + r_1 \tag{18}$$

Rule 2: If (X is A_2) and (Y is B_2) then

$$f_2 = p_2X + q_2Y + r_2 \tag{19}$$

In this paper, ANFIS is trained from the input and output data generated from PID controller.

Layer 1: This consists of input variable membership functions (MFs), input 1 and input 2.Layer 1 provides the input to the layer 2.Bell-shaped MFs with 1 representing maximum and 0 representing minimum values are selected.

Layer 2: The layer 2 checks the weights of each MF .The nodes in layer 2 are non-adaptive and it multiplies the input signals and sends the output as the product of μ_{AB}, μ_{CD} , $W_i = \mu_{AB}(X) * \mu_{CD}(Y)$ where μ_{AB}, μ_{CD} are the membership functions.

Layer 3: Rule layer is the third layer. Each neuron (node) in this layer computes the activation level of each rule, where the numbers of layers are equal to the number of fuzzy rules. The calculated weights in each layer are normalized .The Non-adaptive layer is the third layer and each node determines the ratio of the rules firing strength of each node to the summation of rules firing strengths of all nodes

$$W_i^* = \frac{W_i}{W_1 + W_2} \tag{20}$$

Where i=1, 2. The normalized firing strength is the output of this layer.

Layer 4: The defuzzification layer is the fourth layer .The output values from inference of rules are obtained in this layer.
This layer has adaptive nodes with function

$$0_i^4 = W_i^* * f$$
$$= Wi*(p_iX + q_iY + r_i) \quad (21)$$

Where $\{p_i, q_i, r_i\}$ is the parameter set and in this layer is referred to as consequent parameters.

Layer 5: The layer five forms the output layer which calculates the summation of all inputs from fourth layer and converts the fuzzy classification results into a binary value. It has a single node which calculates the summation of all outputs from defuzzification layer.

The overall output from ANFIS is

$$0i^4 = \sum_i W_i * Xf = \frac{\sum_i W_i f}{\sum_i W_i} \quad (22)$$

Fig.17.shows the ANFIS model for two input single output feed-frontward structure having three hidden layers.

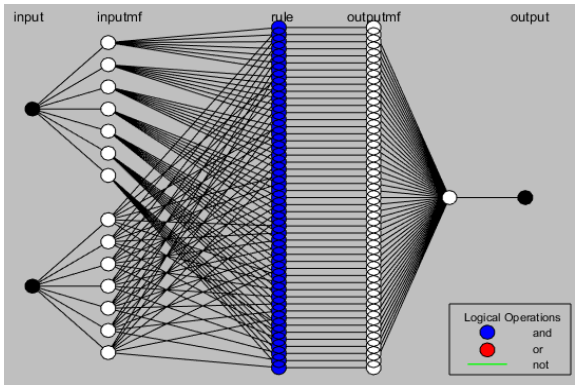

Fig.17. ANFIS structure for the proposed controller.

The proposed method has been implemented using ANFIS editor in MATLAB SIMULINK as shown in Fig. 18.

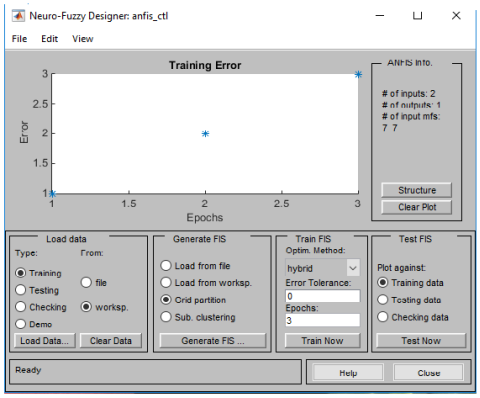

Fig. 18.ANFIS editor

Fig.19. shows the MATLAB Simulink block set for Adaptive Neuro fuzzy PID controller

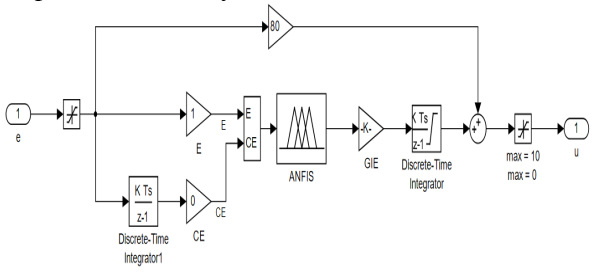

Fig.19.ANFIS implementation using MATLAB Simulink

4. Simulation results and discussions

The circuits are modeled and simulated using the blocks of Simulink and the results with PID controller, Fuzzy controllers and ANFIS controllers are presented here.

The simulation parameters of the wind turbines are: three phase, 1kW, 400V, 50 Hz, Stator resistance of 0.425 ohm, Inductance L_q of 0.0082mH, Inductance L_d of 0.00825mH, Pole pairs of 5, Equivalent moment of inertia of 0.01197kgm^2, Flux induced by magnets of 0.433 Kgm^2.

Meanwhile, the main components and parameters of SEPIC are inductors 1 and 2 are 200µH, Capacitors 1 and 2 are 200µF, 220 µF, diode snubber resistance is 0.001 ohm, and snubber capacitance is 250nF, switching frequency of 25kHz.

The simulations have been done with dynamically varying wind speeds. Initially the wind speed is set as 3m/sec and increased to 12m/sec at t=1 secs.
Fig. 20. Shows the time dependency of the wind speed that was applied to the PMSG Wind Turbine, consequently the controller parameters are varied.

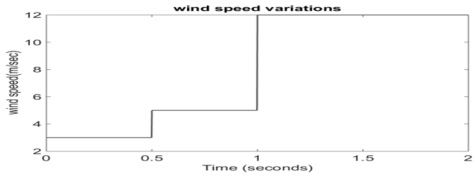

Fig. 20. Wind speed variations

The corresponding variations in PMSG output voltages, SEPIC Output voltage, THD without controller is shown in Figs. 21.1 to 21.3.

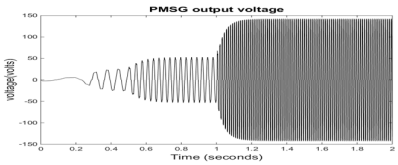

Fig. 21.1. Output voltage of PMSG

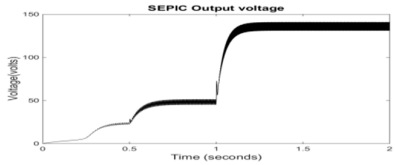

Fig. 21.2. Output voltage of SEPIC(without controller)

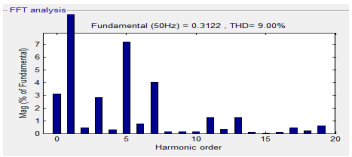

Fig. 21.3.FFT Analysis of Harmonics Level in Output (without controller)

4.1. System with PID controller

Fig. 22. Shows the corresponding FFT analysis waveform. From FFT analysis it is observed that the total harmonic Distortion level in output with PID controller is 6.59%.

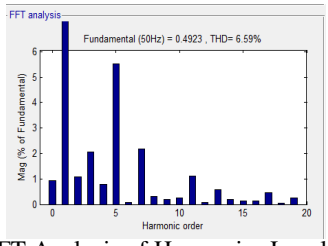

Fig. 22. FFT Analysis of Harmonics Level in Output (with PID controller)

4.2. System with FLC-PID controller

Fig. 23. Shows the corresponding FFT analysis waveform. From FFT analysis it is observed that the total harmonic Distortion level in output with Fuzzy-PID controller is 3.43%.

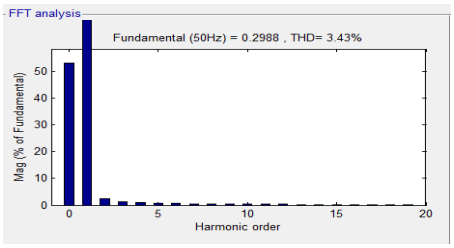

Fig. 23. FFT Analysis of Harmonics Level in Output (with Fuzzy-PID controller)

4.3. System with ANFIS-PID controller:

The output voltages and currents of one phase obtained from the simulation of the SEPIC based wind energy conversion system with the ANFIS controller is shown in Fig. 24.1 and Fig. 24.2.

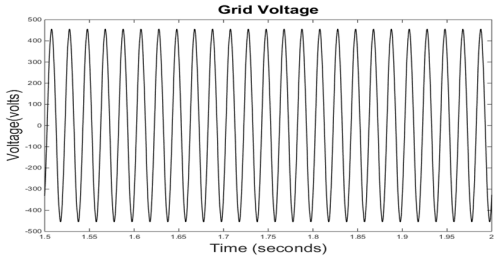

Fig. 24.1. Grid voltage

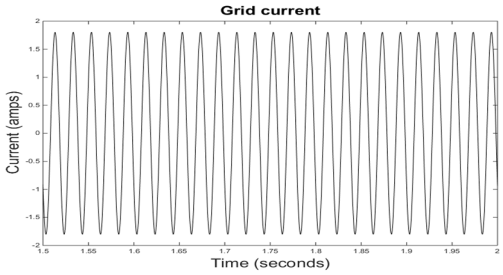

Fig. 24.1. Grid current

The active power, reactive power flow through the load/grid with ANFIS-PID controller is shown in Fig. 25.1 and Fig. 25.2.

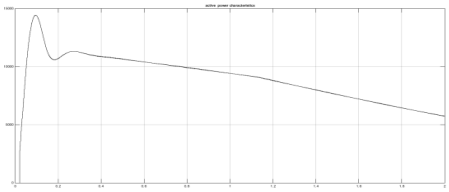

Fig. 25.1. Active power

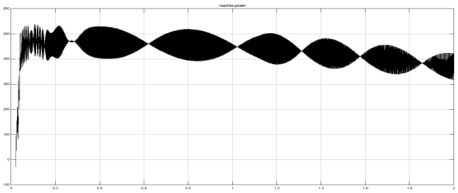

Fig. 25.2. Reative power

Fig. 26. Shows the corresponding FFT analysis waveform. From FFT analysis it is observed that the total harmonic Distortion level in output with ANFIS-PID controller is 0.42%.

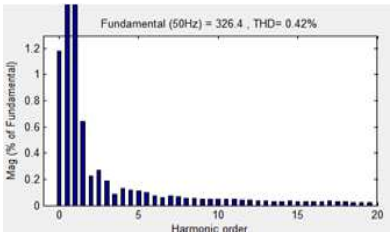

Fig. 26. FFT Analysis of Harmonics Level in Output (with ANFIS-PID controller)

THD obtained from the simulation of SEPIC based wind energy conversion system with and without controllers are compared and shown in the Table 3.

Table 3. Comparison of THD among different methods for tuning a PID controller

Parameter	**Tuning methods**			
	Open loop	**PID**	**FLC-PID**	**ANFIS-PID**
THD	9.00%	6.59%	3.43%	0.42%

The output voltages obtained from the simulation of the SEPIC based wind energy conversion system with the PID, Fuzzy and ANFIS controllers are compared. The comparison of the performance using the PID and Fuzzy logic, ANFIS controllers is summarized in Table 4. For the closed loop SEPIC using FLC-PID the percentage overshoot, Rise time and settling time, steady state error, Total Harmonic Distortion were slightly better than the system using PID controller. Overall it is inferred that the ANFIS-PID controller produces the smoother output with reduced rise time, settling time and peak overshoot, Total Harmonic Distortion.

Table 4. Comparison of dynamic performance among different controllers for tuning a PID

Parameter	**Tuning methods**			
	Open loop	**PID**	**FLC-PID**	**ANFIS-PID**
Rise time t_r(Sec)	0.0345	0.0194	0.0169	0.0128
Settling time t_s (sec)	1.000	1.2000	0.4616	0.1365
Overshoot M_p (%)	4.298	1.9973	1.0985	0.9164

Efficiency obtained from the simulation of SEPIC based wind energy conversion system with and without controllers are compared and shown in the Table 5.

Table 5. Comparison of Efficiency among different methods for tuning a PID controller

Parameter	**Tuning methods**			
	Open loop	**PID**	**FLC-PID**	**ANFIS-PID**
Efficiency	85.6%	87.9%	91.2%	94.3%

5. Conclusion

In this paper, a Variable Speed Wind Energy Generating system (WECS) has been analyzed and the power quality of the system is improved by rectifying its output via Vienna rectifier and converting this into fixed dc using DC-DC SEPIC converter to maintain the inverter input constant and thereby ensuring the power quality of grid tied inverter. This achieved by operating the DC-DC SEPIC converter in closed loop with ANFIS tuned PID controller. The results obtained reveal that the proposed controller reduces the transient characteristics such as settling time, rise time and peak overshoot than the conventional PID and Fuzzy tuned PID controller. Furthermore, the proposed controller improves the efficiency of the system and also reduces the steady state error and overall THD of the system. In addition limitations like distortion in output current, higher ripple and switching stress are overcome by the proposed scheme. The proposed SEPIC using ANFIS-PID based MPPT scheme could be a breakthrough in the real time implementation of variable speed Wind Energy Conversion System.

Reference

1. Muller, S. Deicke M, Doncker R W De.: *Doubly fed induction generator systems for wind turbines. IEEE Ind. Appl. Mag.,* May–Jun.2002,vol. 17, no. 1, pp. 26–33,.

2. Chiang M-H.A *novel pitch control system for a wind turbine driven by a variable-speed pump-controlled hydraulic servo system*. Mechatronics 2011; 21:753–61.

3. Muyeen SM, Al Durra Ahmed, TamuraJ.*Variable speed wind turbine generator system with current controlled voltage source inverter.* Energy Conversion and Management, 2011; 52:2688–94.

4. D. C. Aliprantis, S. A. Papathanassiou, M. P. Papadopoulos, and A. G. Kladas, *Modeling and control of a variable-speed wind turbine equipped with permanent magnet synchronous generator*, in Proc. IEEE Int. Conf. Electrical Machines, Espoo, Finland, Aug. 2000.

5. H. Kim, S. Kim, and H. Ko, *Modeling and control of PMSG-based variable-speed wind turbine*, Electric Power Syst. Res., 2010, vol. 80, pp. 46–52.

6. Rajaei A., Mohamadian M. and Varjani A.Y., (2013), *Vienna-Rectifier-Based Direct Torque Control of PMSG for Wind Energy Application*, IEEE Transactions on Industrial Electronics, 60(7), 2919 - 2929.

7. S. Sivakumar, M.Jagabar Sathik, P.S.Manoj, G.Sundararajan, *An assessment on performance of DC–DC converters for renewable energy applications,* Renewable and Sustainable Energy Reviews, 2016, 1475-1485

8. Kim ID, Kim JY,Nho EC,Kim HG. *Analysis and design of a soft-switched pwm sepic DC–DC converter* .J Power Electron 2010; 10(5):461–7

9. Song Min-Sup, Son Young-Dong, Lee Kwang-Hyun. *Non-isolated Bidirectional soft-switching SEPIC/ZETA converter with reduced ripple currents*. J PowerElectron2014;14(4):649–60.

10.S. Sivakumar a,n, M.Jagabar Sathik b,2, P.S.Manoj c,1, G.Sundararajan b,3 *An assessment on performance of DC–DC converters for renewable energy applications* Renewable and Sustainable Energy Reviews 58, 2016, 1475–1485.

11. L. Guo: *Evaluation of DSP-based PID and Fuzzy controllers for DC–DC converters*, IEEE Trans. Ind. Electron., Jun. 2009, vol. 56, no. 6, pp. 2237–2248,.

12.Shariatpanah H,Fadaeinedjad Rashid inejad M.A *new model for PMSG- based wind turbine with yaw control.*IEEE Trans Energy Convers 2013;24 (8):929–37.

13. Hongyan Zhao, Trillion Q. Zheng , Yan Li , Ji fei Du , and Pu Shi *Control and Analysis of Vienna Rectifier Used as the Generator-Side Converter of PMSG-based Wind Power Generation Systems.* Journal of power electronics 2018

14. Al-Saffar M. A., Ismail E. H., Sabzali A. J. and Fardoun A. A., *An improved topology of SEPIC converter with reduced output voltage ripple,* IEEE Trans. Power Electron. 2008; 23(5): 2377–86

15. Nedijah N, de L, Mourelle M. *Fuzzy systems engineering*: theory and practice. Germany: Springer; 2005.

16. Abraham, A.: *Neuro-Fuzzy Systems: State-of-the-Art Modeling Techniques, Connectionist Models of Neurons, Learning Processes, and Artificial Intelligence*, Springer-Verlag Germany, Jose Mira and Alberto Prieto (Eds.), Granada, Spain, pp. 269-276, 2001.

17. Kalaivani R, Veerapandiyan V, Vidhyasagar D *et.al*.: A New control strategy for PMSG based wind energy conversion system feeding Microgrid, Journal of Electrical Engineering, pp.1-8, 2017.